

MECHANISM OF PINHOLE FORMATION IN MEMBRANE ELECTRODE ASSEMBLIES FOR PEM FUEL CELLS

Vesna Stanic
Teledyne Energy Systems, Inc., West Palm Beach, FL, 33417

Mark Hoberecht
NASA Glenn Research Center, Cleveland, OH, 44135

ABSTRACT

The pinhole formation mechanism was studied with a variety of MEAs using ex-situ and in-situ methods. The ex-situ tests included the MEA aging in oxygen and MEA heat of ignition. In-situ durability tests were performed in fuel cells at different operating conditions with hydrogen and oxygen. After the in-situ failure, MEAs were analyzed with an Olympus BX 60 optical microscope and Cambridge 120 scanning electron microscope. MEA chemical analysis was performed with an IXRF EDS microanalysis system. The MEA failure analyses showed that pinholes and tears were the MEA failure modes. The pinholes appeared in MEA areas where the membrane thickness was drastically reduced. Their location coincided with the stress concentration points, indicating that membrane creep was responsible for their formation. Some of the pinholes detected had contaminant particles precipitated within the membrane. This mechanism of pinhole formation was correlated to the polymer blistering.

INTRODUCTION

Durability of polymer electrolyte membrane (PEM) fuel cells is one of the main problems impeding commercialization of this technology for any application. Reliability of power systems based on PEM fuel cell technology is mostly dependent on membrane electrode assembly (MEA) durability. The probability of PEM fuel cells to replace other energy conversion devices will definitively increase if longer life is verified by achieving durability targets. This is especially important for space applications where safety and reliability are the most important factors. In space applications PEM fuel cells operate on pure hydrogen and oxygen, a very aggressive environment that affects durability drastically. The minimum required life for space applications is 10,000h with other application being much higher. This is still a challenge to be demonstrated at the system level.

The most common failure mode of PEM fuel cells is gas crossover caused by pinhole formation in MEAs. Possible reasons for pinhole formation are material flaws introduced during MEA processing and conditions imposed during fuel cell operation. There are several different explanations reported to date for pinhole causes. One of the earliest attempts to identify them was done by Irvin et al.[1]. They identified small cracks in two areas and correlated their formation to the local membrane shrinkage caused by drying. The membrane drying was caused by limited water transport due to the decomposition of

This is a preprint or reprint of a paper intended for presentation at a conference. Because changes may be made before formal publication, this is made available with the understanding that it will not be cited or reproduced without the permission of the author.

Dacron[®] wicks. In the study performed by La Conti et al. [2] failure of MEAs was assigned to peroxide formation in membranes. Peroxide radicals formed electrochemically in the membrane degraded the polymer, caused its dissolution, and failure. In addition to membrane drying and peroxide attack, the most recent work [3] correlated the surface roughness of gas diffusion layers (GDLs) with the number of pinholes. Stucki et al. [4] demonstrated that pinholes formed not only in PEM fuel cell, but also in PEM electrolyzers. They explained that pinhole formation was caused by membrane dissolution triggered by local stress.

The approach used in this paper was based on assumptions that the membrane aging, excessive heat generated locally, fuel cell configuration (design and components), and operating conditions mutually contribute to the pin hole formation. The objectives were to identify the causes and failure mechanism of pinhole formation by studying the effects of these factors individually. For this purpose the MEA mechanical degradation in oxygen and heat of ignition were studied separately in ex-situ tests, while the effects of operating conditions and fuel cell configurations were evaluated in various fuel cell tests. The MEA failure modes were analyzed by optical and scanning electron microscopes.

EXPERIMENTAL

MEAs studied

For this study MEAs with extruded and cast polymer membranes were used. They were made from 1100EW persulfonated tetrafluoroethylene (Nafion type) polymer. The membrane thicknesses ranged from $\sim 30 \mu\text{m}$ to $170 \mu\text{m}$. The hydrogen and oxygen electrocatalyst was platinum supported on carbon. Gas diffusion layers used were Toray TGHP-90 carbon fiber paper. More than 120 MEAs were tested in ~ 30 fuel cell durability trials.

Ex-situ test procedures

Aging of three different MEAs with cast and extruded membranes was performed in wet and dry oxygen at 70°C and 30psig. They were assembled in a fuel cell and tested without electrical load. Each experiment was carried out for 1000h. They were stopped every $\sim 100\text{h}$ and small MEA samples were cut out for microstructure analysis. When the experiments were completed, the MEA bursting strength was tested [5]. This test was performed on unsupported samples in a specially designed tool. The nitrogen gas was pressurized from one side of the sample at a rate of 20psi/s until it burst.

MEA heat of ignition was determined by a cone calorimeter test [6]. This test measured MEA properties in response to heat and flame under controlled conditions. The properties included heat flux, time to ignite the MEA, and temperature on the MEA surface at ignition. Two MEAs, one with a cast and a second with an extruded membrane, with the same catalyst loadings were tested. The thickness ratio of these two MEAs was $\sim 1:1.8$.

In-situ test procedure

All MEAs selected for this durability study were tested in 4-cell fuel cell stacks with hydrogen and oxygen reactants. More than 30 tests were performed at different operating conditions. To complete tests within a reasonable experimental time, the conditions were selected to accelerate the MEA failure. Assuming that reactant relative humidity is a primary factor determining MEA life, failure location and mode, two accelerated test matrices with different gas inlet relative humidities were generated. One set of accelerated tests was performed with ~ 100% humidified reactants, while the second set was performed with dry gases. The stacks were tested at constant current load. Variables identified in these tests as additional key factors for MEA durability, were changed and implemented in long-term tests.

The stacks were periodically leak checked for gas crossover. The measurements were performed on non-operational stacks at room temperature with nitrogen at 5 psid. When the gas cross over was ~ 10 times MEA intrinsic permeability [7], it was considered that the MEA failed the test.

MEA failure analysis

The MEA microstructures were evaluated after failure in fuel cell tests. Evaluation of failure modes was done on MEA cross sections at the regions weakened during fuel cell operation. Other samples were crushed in liquid nitrogen for cross section analysis.

The analysis of MEA failure modes was performed with an Olympus BX60 optical microscope in different light modes and magnifications. For MEA examination at higher magnifications, a Cambridge Instruments Stereoscan 120 scanning electron microscope was used. Chemical analysis was done with an IXRF EDS 2004 microanalysis system.

RESULTS AND DISCUSSION

MEA Aging in Oxygen

MEA electrocatalyst microstructure changed during tests with dry and wet oxygen. Dry oxygen caused catalyst cracking, while humidified gas increased surface roughness. The changes that occurred during test with dry gas can be explained with MEA shrinkage. MEA components (electrocatalyst layers and membrane) have different shrinkage rates upon drying. Since catalysts layers are more porous, they dry much faster than the polymer membrane. This difference may stimulate the formation and propagation of cracks in catalyst layers. However, MEA swelling in wet oxygen increases electrocatalyst roughness. When the membrane swells its thickness increases. Since it is under constant compression, it fills out voids located on the surface of GDLs. This process creates bulges and indents on the catalyst layer, resulting in rougher surface.

The results of burst tests with MEAs aged in dry and wet oxygen show that the MEA mechanical properties did not degrade during these tests. The burst strength for MEAs with 50 μ m thick cast and extruded membrane is ~ 620 kPa. This result is in agreement

with once previously reported [8] that also indicates the resistance of Nafion type polymers to the chemical attack of oxygen.

MEA heat of ignition

Cone calorimeter test results for two MEAs tested are presented in Table I. The same heat flux was needed to ignite MEAs (1.3 W/cm^2), even though they had different membranes. However, time to ignition was different and proportional to their thicknesses. Thus, the ignition heat of MEA 2 was 1.8 times higher than of MEA 1.

Table I: Critical heat flux and ignition heat and temperature for two MEAs tested.

MEA	MEMBRANE	THICKNESS (μm)	HEAT FLUX (W/cm^2)	TIME TO IGNITION (Seconds)	IGNITION HEAT (Ws/cm^2)	TEMPERATURE AT IGNITION ($^{\circ}\text{C}$)
1	CAST	T	1.3	6.81	8.85	296
2	EXTRUDED	1.8 T	1.3	12.55	16.31	297

Assuming that MEA ignition heat is mostly determined by polymer membrane, and not by catalyst layers, the polymer heat capacity was calculated from the ignition heats (Table I) and corresponding membrane weights. The heat capacity calculated at room temperature and ambient pressure for both cast and extruded polymer membranes was the same $735\text{J/g}\cdot\text{K}$.

When ignition heat of MEAs is compared to the heat generated during fuel cell operation at test conditions used, it is one to two orders of magnitude higher than the heat generated in fuel cell. For instance, a typical heat loss of MEA 1 is 0.13 W/cm^2 . If there is no heat loss by cooling or water evaporation, then the heat generated in fuel cell is ~ 70 times lower than the heat necessary to ignite MEA 1. This result indicates that heat generated locally at the MEA active sites is not high enough to create instantly a hotspot. For thicker MEA 2 this heat ratio is even higher, ~ 120 .

MEA failure analysis

The results of MEA microstructure analyses after fuel cell tests showed that the MEA failure modes were pinholes and tears. These defects were localized and usually aligned along the channel edges. The failure location depended on operating conditions and fuel cell configurations, and not on MEA type and thickness. When different MEAs were tested in accelerated tests with humidified gases in fuel cells with the same configuration, the location of defects was always the same. However, when fuel cell configuration was changed, the failure location shifted to a different area.

Accelerated tests with dry gases were carried out with the same MEAs and fuel cell configurations, however at different operating conditions. In these tests, failure locations changed from test to test. Modeling of relative humidity distribution across the MEA active area showed that the failure locations in tests with humidified and dry gases coincided with areas close to the reactant inlets. Since the electrochemical reaction rate is proportional to the gas concentration, the MEAs have higher reaction rates at these locations. The higher reaction rates increase local current densities and further generate more heat, resulting in MEA localized failure.

A typical MEA pinhole is presented in Fig.1. The SE micrograph shows that the $\sim 20 \mu\text{m}$ hole in the membrane is surrounded with burned catalyst. Black lines in the micrograph present carbon fiber indentations in the MEA catalyst layer. These indents were created in the catalyst layer after MEA assembly in fuel cell as a result of compression and swelling.

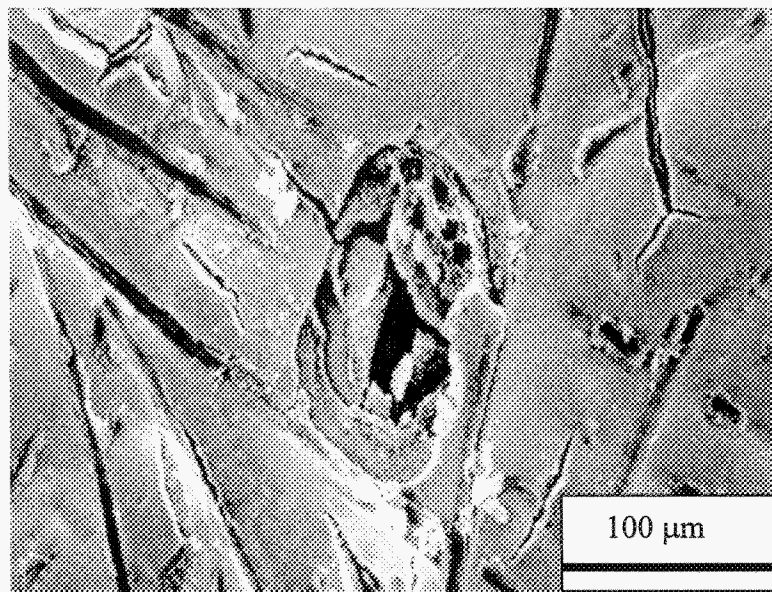


Figure 1: A typical pinhole in MEA cathode catalyst layer. The pinhole is $\sim 20 \mu\text{m}$ wide and surrounded with burned catalyst. Lines in micrograph are carbon fiber indentations.

Tears in MEAs are created when an MEA is taken out of a fuel cell and exposed to ambient conditions. Shrinkage due to drying in air at room temperature places the MEA under tension. This force is high enough to tear the MEA only at these weakened areas. The SEM analysis of fractured surfaces of tears indicated that they had aligned pinholes, thin spots, cracks, and contaminants. Cracks, thin spots and contaminants are the MEA damages that precede the pinhole genesis. The tear analyses indicate that membrane creep and contaminant precipitation within the membrane cause pinhole formation.

Pinhole formation by Creep

The SEM of the MEA cross sections before and after fuel cell test are presented in Fig.2. The MEA presented has an extruded membrane. The micrograph in Fig. 2a shows that the new MEA has uniform thickness. However, after fuel cell test with humidified gases the membrane thickness is reduced and non-uniform (Fig. 2b). Even though this SEM sample is taken from the MEA area free of damages, the membrane thickness is reduced by 40%. In addition, the membrane thickness variations occur equally on both anode and cathode sides and coincide with the GDL surface roughness.

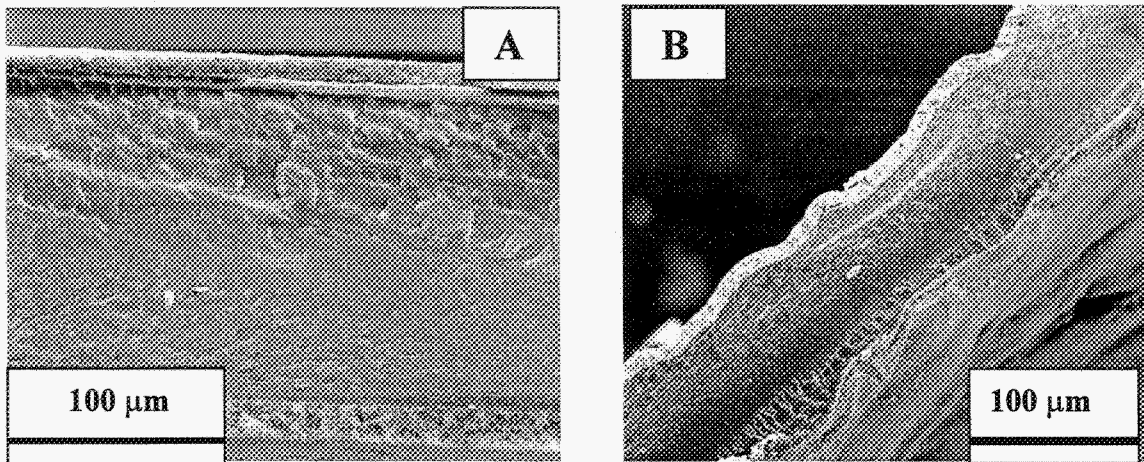


Figure 2: Scanning electron microscope of cross section of MEA with extruded membrane: A) new MEA; B) MEA thickness is reduced by 40% and non-uniform after fuel cell test.

Microstructure analysis of MEAs tested with dry gases show that membrane thickness is also reduced under these conditions. On the other hand, the thickness non-uniformity is less apparent at the microscopic scale, indicating lack of membrane swelling in a dry fuel cell environment.

The membrane thickness reduction (thinning) indicates that the polymer membrane experiences mechanical degradation due to creep when exposed to thermal and mechanical loadings in the fuel cell. Polymers, including Nafion type membranes, are viscoelastic materials and their mechanical properties are time and temperature dependant. When polymers are subjected to constant load, the elastic modulus progressively decreases with time [9], since the polymer molecules reorganize to minimize localized stresses. Molecular reorganization includes stretching, slip, and even molecular scission if intense localized stresses are applied. This polymer response to long-term creep leads to the change of cross sectional area which in turn results in polymer failure when it can no longer accommodate the applied stress.

The results of MEA failure by creep are pinholes. The mechanism of their formation is affected with the membrane type and humidity level they are exposed to in the fuel cell. There are two mechanisms caused by creep. The first implies extruded membranes at any humidity and cast membranes tested with dry gases undergo creep rupture. This type of

creep failure involves crack development when the critical thickness reduction is reached. It is found that this critical number is 75% for both extruded and cast membranes. Cracks detected in fractured surfaces of tears in both extruded and cast membranes are generated on anode side. They continue to propagate under constant stresses as presented in Fig.3a, and eventually create a leak path for the gases. Since hydrogen and oxygen chemical reaction is highly exothermic (285 kJ/mole of hydrogen), heat produced even with small hydrogen crossovers can ignite the MEA. Thus, to create a pinhole in an extruded membrane presented in Fig. 3b, a hydrogen flow rate should be only $6.2 \cdot 10^{-6} \text{ cm}^3/\text{s}$. This flow rate is calculated based on the pinhole size and MEA ignition heat (Table I).

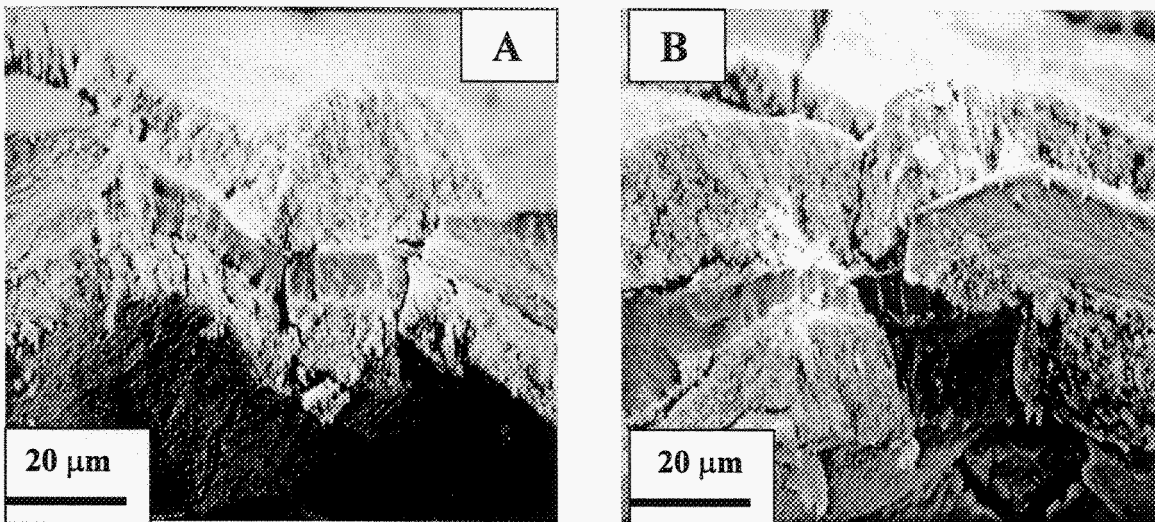


Figure 3: Scanning electron microscope of fractured surface of tear in MEA. This MEA has extruded membrane and is tested with humidified gases: A) two cracks propagated from anode to cathode side. The membrane thickness is reduced by 80% at this spot; B) A pinhole in the same MEA

The second mechanism of pinhole formation by creep that occurs in cast membranes tested with humidified gases is caused by membrane thickness reduction (thinning). The results of microstructure analysis showed that membrane thickness decrease by 90% before it collapses. Spots only $5 \mu\text{m}$ thick are detected in a cast membrane. When membrane collapses it becomes too thin, and is no longer a barrier to the mixing of gases. They react chemically and create a pinhole.

The failure analysis of MEAs show that tears and pinholes are localized. Fuel cell experimental results indicate that they appear in areas where the MEA is mechanically and thermally overstressed. The anisotropic compression and heat distribution in fuel cell at the macroscopic level, caused by improper stack configuration and water management, create MEA areas that are more active and thus generate more heat. Any imperfection that exists in the MEA on the microscale results in pinhole formation. The reason for this is the acceleration of creep [10]. Thus, locations that operate under higher compression and temperature fail faster. Stress concentration points in the MEA may be caused by GDL surface roughness, broken carbon fibers, or debris localized at the MEA/GDL

interface. This over compression decreases membrane thickness that further results in the local conductivity, current, and heat increase. Therefore, over compression increases temperature, and they mutually accelerate creep.

Pinhole formation due to contaminants

In addition to MEA failure caused by membrane creep, MEAs also failed due to contaminants precipitated within the membrane. The scanning electron micrographs shown in Fig. 4, present the MEA cross section with contaminant particles. The micrographs are taken from the fractured surface of a tear. The micrograph in Fig. 4a shows a spot with contaminant particles within the membrane. This spot is located in one oxygen inlet channel. The micrograph shows that contaminants accumulate in the middle of the membrane and grow as monocrystalline particles with similar sizes. These particles are located in one plane within a large blister. Similar, but smaller blisters (20 – 300 times) are also observed along the tear between the adjacent oxygen inlet channels (Fig. 4b). However, the contaminant particles are not observed within them.

The analysis of a tear at the hydrogen inlet shows that fewer numbers of monocrystals precipitated within the membrane (Fig. 4b). Each particle grew individually at the sites isolated by polymer. Their sizes are similar to the particles in the oxygen inlets (~12 μ m).

Potential sources of contaminants coming into the fuel cell are the upstream system and stack components in contact with liquid water. The contamination of the MEA may have a significant effect on fuel cell performance since it can lead to both kinetic and ohmic potential losses [11]. Fundamental studies addressing this issue revealed that catalyst poisoning increases kinetic loss while proton displacement by larger cations in the membrane increases the resistive loss.

Even though MEA contamination was a reason for pinhole formation, the fuel cell activation and ohmic losses were immeasurable. Indeed, they demonstrated a voltage increase of 20 μ V/h. The voltage increase was directly proportional to the MEA resistance decay. The resistance dropped from 0.983 Ω cm² to 0.943 Ω cm². This result indicated that the membrane contaminants were located in narrow zones along the channels where the MEA failed.

The results of EDX chemical analysis of contaminant particles demonstrate that they contain a metal oxide. Divalent cation M^{2+} is leached out by liquid water that comes into contact with a contaminant source. The M^{2+} replaces H^+ in the membrane and makes the crystal nucleation sites with $-SO_3^-$. Since the sulfonic ($-SO_3^-$) groups are fixed to the polymer molecules, they cannot participate in the crystal growth. Thus, the metal oxide crystallites continue to grow within the membrane being constantly supplied by M^{2+} from liquid water and oxygen from the gas stream. In the areas where the cation concentration is higher, such as the inlet channels of oxygen and hydrogen, the crystals are much larger than along the channels where the cation concentration is depleted.

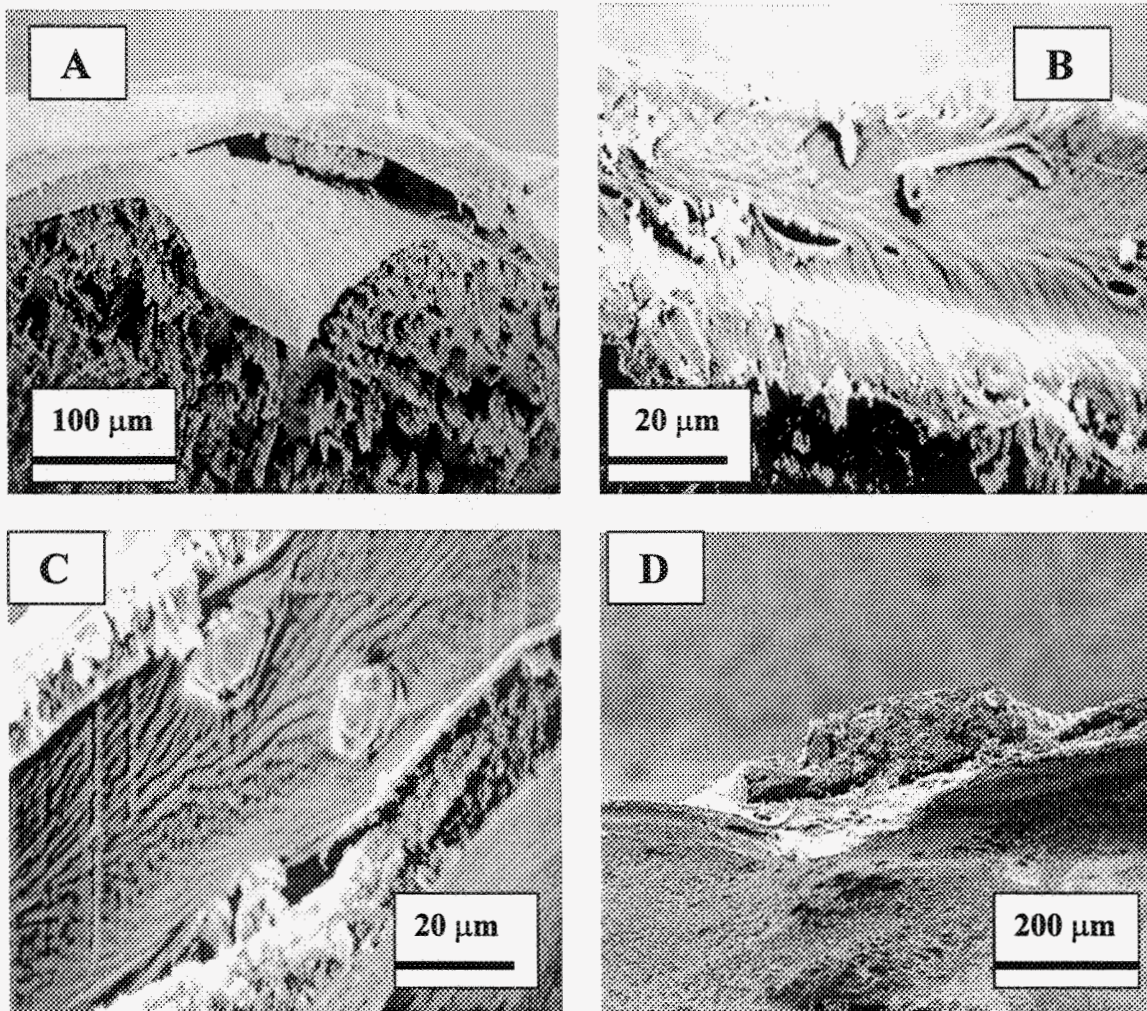


Figure 4: Scanning electron micrographs of contaminant particles and blisters in MEA: a) particles precipitated within the membrane created a large blister in the oxygen inlet channel; b) small blisters in the membrane; c) two small contaminant particles in the hydrogen inlet channel; d) pinhole created due to contaminant precipitation and membrane blistering.

The presence of contaminant particles in the membrane causes blister formation. Blistering is a well-known polymer failure mechanism [9] and can also be used to explain the pinhole formation in Nafion type membrane. The particles that exist within the membrane create small voids around them. These voids are filled with liquid water. When the cell is heated from room temperature to the fuel cell operating temperature, the water vapor partial pressure increases in these voids, and expands them. Since the processes of the particle and blister growth are continuous, the small blisters (Fig. 4b) will eventually coalesce and form large ones (Fig. 4a). Large blisters such as this, allow gas permeation and mixing that results in their chemical reaction and pinhole formation (Fig. 4d).

Therefore, pinhole formation via chemical failure mechanism occurs through several steps that include contaminant leach out by liquid water, particle nucleation and growth within the membrane, and membrane blistering. Blisters weaken the mechanical properties of MEAs causing them to fail at these points.

CONCLUSIONS

Failure analyses of MEAs indicate that mechanical and chemical changes in MEA cause pinholes. The mechanical changes are related to the membrane creep. Depending on the membrane type and humidification level in fuel cell tests, two different mechanisms of pinhole formation by creep are identified. The first mechanism includes crack development and propagation that leads to the reactant gas crossover. This mechanism is typical for extruded membranes at any humidity condition as well as cast membranes at dry conditions. The creep of cast membranes tested with humidified gases results in a different mechanism. It involves the reduction of membrane cross sectional thickness until it no longer acts as a gas barrier.

Accelerated durability tests with dry and humid hydrogen and oxygen suggest that anisotropic distribution of compression and heat across the MEA active area causes failures. These non-uniform conditions are the result of the fuel cell configuration and operating conditions. However, the stress concentration points localized at the MEA/GDL interface cause compression and heat variation on the microscopic level. When their effect is superimposed on the heat and compression variations on the macro scale, then pinholes are created in localized areas of MEA.

In addition to pinholes created by creep, some are formed due to MEA chemical failure. This failure is a consequence of proton replacement in the polymer membrane with larger cations leached out with liquid water from the fuel cell or system components. This mechanism of pinhole formation occurs through several steps. The first step includes contaminant particle nucleation and growth within the membrane from cations and oxygen provided with fluid streams coming into the fuel cell. When they begin to form, the particles are surrounded with small voids. During fuel cell thermo cycles, these voids enlarge and create blisters. Blisters create a path for gases to crossover and mix.

The weak spots in membrane created by either mechanical or chemical failure mode, such as cracks, thin spots or blisters, allow gas mixing. The chemical reaction of hydrogen and oxygen generates enough heat to melt the polymer, burn the catalyst and form a pinhole in MEA.

ACKNOWLEDGEMENT

The authors gratefully acknowledge the financial support of NASA Glenn Research Center (contract # NAS 3-02093 and NAS 3-02203).

REFERENCES

1. L. F. Irvin, *Evaluation of an Ion Exchange Membrane Fuel cell For Space Power*, (1974) p. 1-13.
2. A. B. La Conti, A.R. Fragala, and J. R. Boyack, in *Proceedings of the Symposium on Electrode Materials and Processes for Energy Conversion and Storage*, J. D. E.

- Mcintyre, S. Srinivasan, and F. G. Will, Editors, p.354, The Electrochemical Society Proceeding Series, Princeton, NJ (1977).
3. V. Peinecke, J. von der Osten-Fabeck, J. R. Gordon, H. R. Haas, US Patent 6,716,551, April 6, 2004.
 4. S. Stucki, G. G. Sherer, S. Schlagowski, E. Fischer, *J. Applied Elchem.*, **28**, 1041 (1998).
 5. ASTM D3662.
 6. ASTM E-1354-97
 7. J. L Larminie, A. Dicks, *Fuel cell Systems Explained*, p.47, John Wiley & Sons, Ltd., Chichester (2000).
 8. S. Stucki, G. Theis, R. Kötzt, H. Devantay, H.J. Christen, *J. Electrochem. Soc.*, **132**, 1041 (1985).
 9. J. Scheirs, *Composition and Failure Analysis of Polymers*, p. 315, John Wiely & Sons, Ltd., New York (2000).
 10. D. R. Askeland, *The Science and Engineering of Materials*, p.488, PWS Publishing Company, Boston (1994).
 11. J. St-Pierre, D.P. Wilkinson, S. Knights, M.L. Boss, *J. New Mat. Electrochem. Systems*, **3**, 99 (2000).

Keywords: MEA pinholes, MEA durability, Pinhole formation, PEM durability